

Magnesium–Adenosine Diphosphate Binding Sites in Wild-type Creatine Kinase and in Mutants: Role of Aromatic Residues Probed by Raman and Infrared Spectroscopies[†]

Hans Hagemann,[‡] Olivier Marcillat,[§] René Buchet,^{*,||} and Christian Vial[§]

Département de Chimie Physique, Université de Genève, Sciences II, 30 quai Ernest-Ansermet, CH-1211 Genève 4, Switzerland, et Biomembranes et Enzymes Associés et Laboratoire de Physico Chimie Biologique, Université Claude Bernard—Lyon I, UFR de Chimie—Biochimie, CNRS UMR 5013, F-69622 Villeurbanne France

Received January 4, 2000; Revised Manuscript Received April 11, 2000

ABSTRACT: Two distinct methods were used to investigate the role of Trp residues during Mg-ADP binding to cytosolic creatine kinase (CK) from rabbit muscle: (1) Raman spectroscopy, which is very sensitive to the environment of aromatic side-chain residues, and (2) reaction-induced infrared difference spectroscopy (RIDS) and photolabile substrate (ADP[Et(PhNO₂)]), combined with site-directed mutagenesis on the four Trp residues of CK. Our Raman results indicated that the environment of Trp and of Tyr were not affected during Mg-ADP binding to CK. Analysis of RIDS of wild-type CK, inactive W227Y, and active W210,217,272Y mutants suggested that Trp227 was not involved in the stacking interactions. Results are consistent with Trp227 being essential to prevent water molecules from entering in the active site [as suggested by Gross, M., Furter-Graves, E. M., Wallimann, T., Eppenberger, H. M., and Furter, R. (1994) *Protein Sci.* 3, 1058–1068] and that another Trp could in addition help to steer the nucleotide in the binding site, although it is not essential for the activity of CK. Raman and infrared spectra indicated that Mg-ADP binding does not involve large secondary structure changes. Only 3–4 residues absorbing in the amide I region are directly implicated in the Mg-ADP binding (corresponding to secondary structure changes less than 1%), suggesting that movement of protein domains due to Mg-nucleotide binding do not promote large secondary structure changes.

Creatine kinase (CK)¹ isoenzymes participate in the regulation of ATP supply during contraction of muscle or other high-energy metabolic process (1–3). The different localization of isoenzymes and substrates in the cells suggested distinct roles for the mitochondrial CK and the cytosolic CK (4). The mitochondrial CK, in the vicinity of ATP production site, converts creatine into phosphocreatine, while cytosolic CK (MM isoenzyme of creatine kinase), found in myofibrils, functions as a fast energy supplier by converting phosphocreatine and ADP into creatine and ATP. This regulation mechanism, the so-called creatine–phosphocreatine energy shuttle (4), explains that during muscle contraction, ATP levels are only minimally decreased while creatine phosphate is depleted. Despite their different functional roles in ATP regulation, octameric mitochondrial

CK and dimeric cytosolic CK can both catalyze reversibly the transfer of phosphoryl group from adenyl substrates to guanidino derivatives. Their protein sequences and gene structures are similar (5–7). The X-ray structures of octameric mitochondrial CK isoform (8) and of dimeric cytosolic CK (9), as well as of monomeric arginine kinase (10), share the same subunit topology. Each monomer has a small α -helical N-terminal domain and a large C-terminal domain containing eight-stranded antiparallel β -sheet flanked by seven α -helices. The X-ray resolved structures provided detailed insights into the active site (8) and into the importance of precise substrate alignment in the catalysis of bimolecular reactions (10).

In this respect, Trp residue could contribute for restraining the freedom of substrates and for steering the reactants toward the active site. Several experimental results support this hypothesis: (A) ultraviolet absorption spectroscopy of CK indicated that a Trp residue is near the active site (11–13); (B) near-ultraviolet rotatory dispersion spectra of complexes of rabbit skeletal muscle CK with ATP or ADP suggested stacking of purine of adenine moiety on one aromatic group of the enzyme (14); (C) fluorescence measurements of rabbit skeletal muscle CK (15–20) identified a tryptophanyl residue close to the active site; and (D) site-directed mutagenesis of chicken sarcomeric mitochondrial creatine kinase indicated that substitution of Trp223 by Phe resulted in more than 96% inactivation (21). Total

[†] This work was supported by the Swiss National Science Foundation and the Region Rhône Alpes.

^{*} To whom correspondence should be addressed at Université Claude Bernard—Lyon I, UFR de Chimie—Biochimie, 43 Boulevard du 11 Novembre 1918, F-69622 Villeurbanne, France. Fax +33 4 72 43 15 43; phone +33 4 72 43 13 20; e-mail rbuchet@cismibm.univ-lyon1.fr.

[‡] Université de Genève.

[§] Biomembranes et Enzymes Associés, Université Claude Bernard—Lyon I.

^{||} Laboratoire de Physico Chimie Biologique, Université Claude Bernard—Lyon I.

¹ Abbreviations: CK, creatine kinase; FTIR, Fourier transform infrared spectroscopy; RIDS, reaction-induced infrared difference spectrum.

inactivation was also observed for cytosolic CK from rabbit muscle when the corresponding residue Trp227 was replaced by a Tyr residue (22).

The objective of this work was to substantiate the roles of tryptophan residues upon adenylate binding. We used two complementary approaches: (A) Raman spectroscopy, which can reveal detailed information on Trp and Tyr side-chain environment (e.g., refs 23–25), and (B) site-directed mutagenesis on cytosolic CK in conjunction with activity measurements and infrared spectroscopy. The sequence of rabbit muscle CK contains four Trp residues located respectively at positions 210, 217, 227, and 272. Since Trp227 residue was essential to the activity of CK but did not abolish completely ADP binding infrared changes, the other Trp residues such as Trp210, Trp217, and Trp272 were replaced by Tyr residues so that their putative roles in the Mg-ADP binding could be monitored by use of reaction-induced infrared difference spectroscopy (RIDS) and photolabile caged ADP (26, 27).

MATERIALS AND METHODS

Chemicals. Tris, monopotassium salt ADP ($C_{10}H_{14}N_5O_{10} \cdot P_2K \cdot 2H_2O$), and phenylmethanesulfonyl fluoride (PhMeSO₂F) were purchased from Boehringer. The photolabile caged ADP, ADP[Et(PhNO₂)], was obtained from Molecular Probes Europe.

Preparations of Solutions for Raman Spectra. CK [protein dimer concentration ranging from 115 μ M (10 mg mL⁻¹) to 230 μ M (20 mg mL⁻¹)] without or with Mg-ADP (1.7 mM) was dissolved either in normal water buffer solution (10 mM Tris-HCl, pH 6.5–7.8, and 10 mM MgCl₂) or in deuterated buffer solution (10 mM Tris-HCl, p²H 7–7.5, and 10 mM MgCl₂). Buffers without CK in the absence or presence of Mg-ADP (from 1 to 2 mM) were prepared under the same conditions as for samples containing CK. To prevent nonspecific nucleotide binding at high nucleotide concentration, it was suggested to use nucleotide concentration around 1.5 mM and CK dimeric concentration around 180 μ M (28). These conditions match closely ours and therefore weak nonspecific binding sites can be considered as negligible. Raman measurements were performed at room temperature (21 °C) on a laboratory-assembled Raman spectrometer consisting of the following parts: a Spectra Physics argon ion laser (model 2060-5 Beamlok, supersilent option) and a Kaiser Holospec f/1.8 spectrograph equipped with a Princeton Instruments liquid nitrogen-cooled CCD camera (LN CCD 1752 PB). This setup is computer-controlled with software developed in the laboratory. Sample solutions were contained in 5 × 5 mm quartz fluorescence cells. All spectra were excited with the 488 nm laser line with a power of 0.25 W. The unpolarized measurements were obtained in a 90° scattering geometry. With a 25 μ m slit, the spectral resolution was ca. 3–4 cm⁻¹. Exposure times ranged from 15 to 50 s; up to 150 exposures were coadded for improved signal-to-noise ratio. For creatine kinase in solution, the total exposure time was typically 3000 s. The buffer solvent spectrum (obtained under identical experimental conditions) was subtracted from the spectra. For better clarity in the figures, the background was corrected by use of only a single straight line for the entire region displayed. No filtering or smoothing was applied to the data. Curve-fitting with

Lorentzian line shapes was performed to estimate relative peak heights.

Tryptophan Fluorescence Spectra. Creatine kinase fluorescence emission spectra were taken at 20 °C with a Hitachi F4500 spectrofluorometer. Excitation was set at 295 nm in order to decrease as much as possible tyrosine excitation. Spectra were recorded with 2.5 μ M protein dimer concentration (0.22 mg mL⁻¹) in 10 mM Tris-HCl, pH 7.5, and 10 mM MgCl₂ buffer without and with 1.7 mM ADP-Mg. Spectra are corrected from solvent background and for ADP inner filter effect (29).

Expression and Mutagenesis of MM-CK. Muscle-type CK subunit was expressed and purified as described (30). Replacement of tryptophan residues by tyrosine was achieved by site-directed mutagenesis (31) of the pET-MM phagemid. The complete coding region of the resulting mutant was checked by dideoxy sequencing. Mutant proteins were expressed and purified as described (30).

Preparation of Mutant in Solutions for the Infrared Measurements. W210,217,272Y mutant was lyophilized and excess salts were removed by washing with ²H₂O buffer (100 mM Tris-HCl, p²H 7.5, 10 mM MgCl₂, and 1.3 mM dithiothreitol) and use of a Centricon filter. After four washing steps, W210,217,272Y mutant was dissolved in ²H₂O buffer containing 100 mM Tris-HCl, p²H 7.5, 10 mM MgCl₂, and 1.3 mM dithiothreitol with and without 2 mM ADP[Et(PhNO₂)]. The final protein dimer concentration was 94 μ M (8.2 mg of protein/mL). The p²H was determined with a glass electrode and was corrected by a value of 0.4 (32). Buffer without protein (100 mM Tris-HCl, p²H 7.5, 10 mM MgCl₂, and 1.3 mM dithiothreitol with and without 2 mM ADP[Et(PhNO₂)]) was also used to determine their infrared absorptions. The samples were freshly prepared and incubated for 60 min in the dark at room temperature before FTIR measurement.

Reaction-Induced Infrared Difference Spectroscopy. Infrared spectra of W210,217,272Y mutant were measured by means of a Nicolet 510M FTIR spectrometer equipped with a DTGS detector, with a temperature-controlled flowthrough cell (model TFC-M25; Harrick Scientific Corp., Ossining, NY). The cell path length was 50 μ m and windows were CaF₂. Typically, the infrared spectra were recorded at 25 °C with 256 interferograms each at 4 cm⁻¹ resolution, Fourier-transformed. During data acquisition, the spectrometer was continuously purged with dry filtered air (Balston regenerating desiccant dryer, model 75-45 12 VDC). Once the infrared spectrum was recorded, each sample was exposed to 30 s of ultraviolet illumination that induced the photorelease of active ADP from inactive ADP[Et(PhNO₂)], allowing ADP binding to the mutant. After this illumination, a second FTIR spectrum was again recorded under the same conditions. The reaction-induced difference spectrum (RIDS) of the sample was obtained by subtracting the first FTIR spectrum (before illumination) from the second FTIR spectrum (after illumination). Thirteen RIDS, obtained from three independent preparations, were measured under the same conditions and were coadded to obtain the final RIDS with better signal-to-noise ratio. The final RIDS was corrected for water vapor absorption but was not smoothed. The corresponding RIDS of wild-type CK and of W227Y, reported previously (33), were used to collate the different RIDS. They were measured under similar conditions except

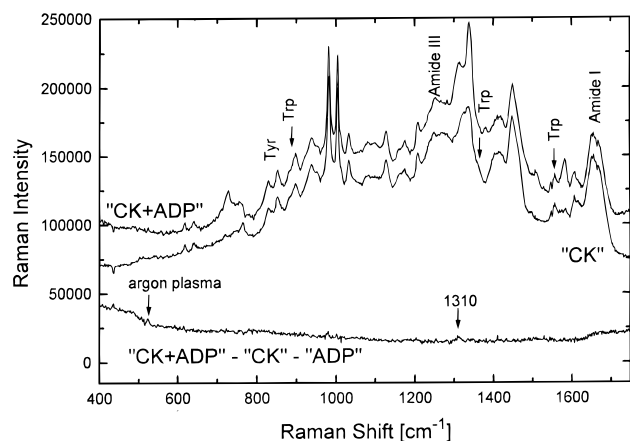


FIGURE 1: Raman spectra of Mg-ADP-CK complexes in normal buffer. From top to bottom: trace 1, Raman spectrum (solvent-subtracted) of creatine kinase (115 μ M protein dimer concentration in 10 mM Tris-HCl, pH ca. 6.5, and 10 mM MgCl_2) in the presence of Mg-ADP (1.7 mM) (CK + ADP); trace 2, Raman spectrum (solvent-subtracted) of creatine kinase (CK); trace 3, Raman difference spectrum, trace 1 (CK + ADP) minus trace 2 (CK) minus Raman spectrum of ADP (1.7 mM).

that their protein dimer concentrations were 115 μ M (10 mg of protein/mL).

RESULTS

Raman Spectra of Native Creatine Kinase. The Raman spectrum of native CK in buffer (10 mM Tris-HCl, pH 7.8, and 10 mM MgCl_2) is shown in Figure 1. Line fitting of the Tyr doublet at 852 and 828 cm^{-1} yields an intensity ratio (peak height) $I(852)/I(828)$ of 1.25, suggesting that Tyr acts as weak H-bond donor/acceptor (34). The Raman spectra around 900 cm^{-1} show basically two bands at ca. 880 and 900 cm^{-1} but no band close to 870 cm^{-1} . According to the literature (35) this indicates that Trp is rather free from hydrogen bonding or inaccessible to solvent. Around 1350 cm^{-1} , there is a strong overlap with CH_2 and CH bands, but nevertheless a shoulder around 1365 cm^{-1} can clearly be seen, which was assigned to Trp residue located in a hydrophobic surrounding (36). A further indole ring vibration is observed at 1556 cm^{-1} . This vibrational mode is related to the C2-C3-C α -C β torsional angle, i.e., the orientation of the indole ring with respect to the C α atom of the amino acid backbone. Position of this band is very sensitive to torsional angle. In the present case, this angle is estimated to be close to 100°. It has been noted previously (23) that the band located at 1556 cm^{-1} lies close to the one observed (1553 cm^{-1}) for free Trp, giving rise to a torsional angle of 100° (37).

Spectral Changes Induced by the Addition of Mg-ADP to CK. The Raman difference spectrum in Figure 1 shows that there are very small changes that appear upon addition of Mg-ADP to the creatine kinase solution. Only a very weak positive band at 1310 cm^{-1} can be distinguished. Otherwise, we do not observe any significant change for any creatine kinase mode in the entire spectral range from 400 to 1750 cm^{-1} . The measurements of Raman spectrum of CK in deuterated solvent confirm these observations. Raman spectra of CK in normal buffer at pH ca. 6.5 and at pH = 7.8 yield very similar results, confirming that CK is stable above pH = 6 (38). Although Raman spectra did not indicate significant

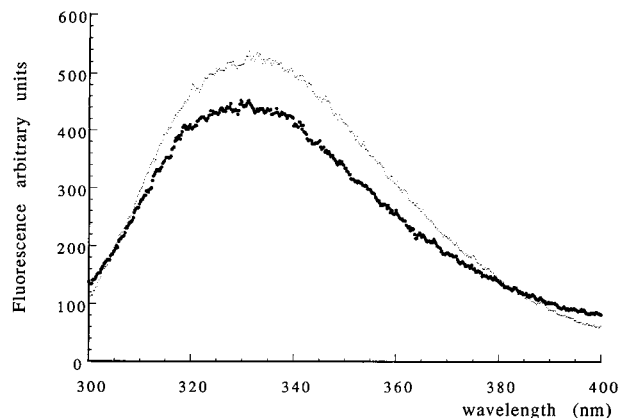


FIGURE 2: Fluorescence spectra of CK in the absence and in the presence of Mg-ADP. Intrinsic fluorescence spectra of CK in 10 mM Tris-HCl, pH 7.5, and 10 mM MgCl_2 buffer without (thick trace) and with (thin trace) 1.7 mM ADP-Mg. Protein dimer concentration was 2.5 μ M. Spectra are corrected from solvent background and from the ADP inner filter effect.

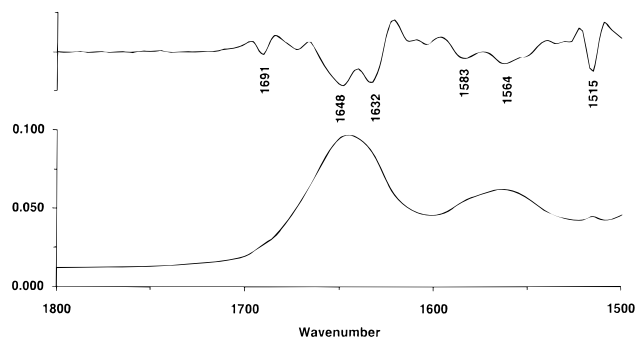


FIGURE 3: Infrared spectrum of W210,217,272Y mutant in deuterated buffer. The bottom trace shows the infrared spectrum of 94 μ M W210,217,272Y mutant in $^2\text{H}_2\text{O}$ buffer (100 mM Tris-HCl, pH 8, 10 mM MgCl_2 , and 1.3 dithiothreitol) after deduction of the infrared absorption of buffer. The top trace represents its second-derivative spectrum.

changes caused by ADP binding to CK, intensity of intrinsic Trp fluorescence is affected upon ADP binding (Figure 2).

Infrared Spectrum of W210,217,272Y Mutant. To precisely identify the role of Trp residues, we have performed site-directed mutagenesis on Trp residues of CK, measured the activity of each mutant, and probed its secondary structure changes induced by Mg-ADP binding. W210,217,272Y mutant of CK has about 41% the activity of the wild type of CK as measured by the pH-stat method (39). The bottom trace in Figure 3 shows a part of infrared spectrum of W210,217,272Y mutant (8.2 mg of protein/mL in $^2\text{H}_2\text{O}$ buffer containing 100 mM Tris-HCl, pH 8, 10 mM MgCl_2 , and 1.3 mM dithiothreitol). The top trace in Figure 3 indicates its second derivative. The second-derivative spectrum allowed to better locate component bands that were not well resolved in the original spectrum. At least three component bands located at 1691, 1648, and 1632 cm^{-1} appeared in the amide I region. The 1648 cm^{-1} band is highly characteristic of α -helix structure, while the pair located at 1691 and 1632 cm^{-1} could correspond to β -sheet structures (40-42). Usually the higher-wavenumber band of the pair is smaller in intensity than the lower-wavenumber band. The putative assignment of the pair of bands to β -sheet structures is consistent with the observed band shape of the infrared spectrum (Figure 3). Other vibrational modes belonging to

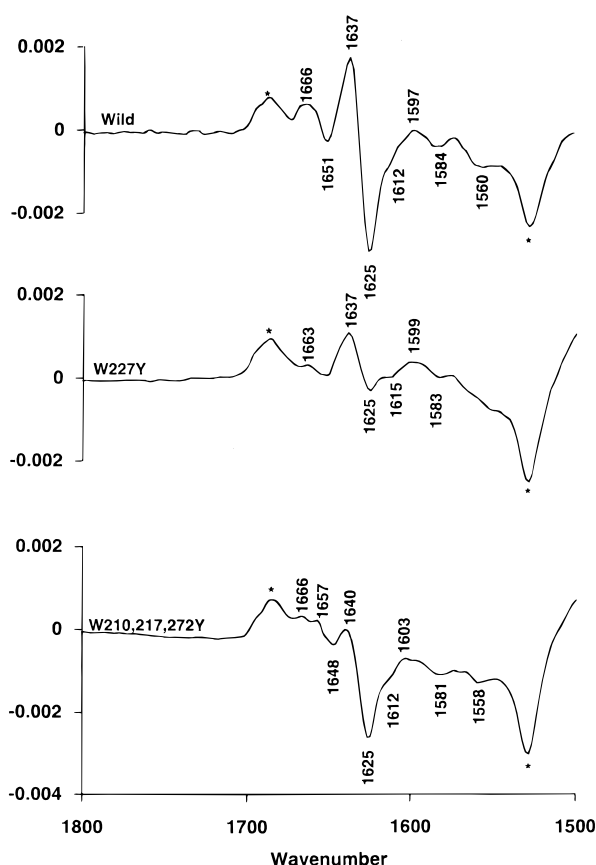


FIGURE 4: Difference infrared spectra induced by the photorelease of ADP from ADP[Et(PhNO₂)] in ²H₂O buffer containing wild-type and mutant CK. Top trace: RIDS of 115 μ M wild-type CK in ²H₂O buffer (100 mM Tris-HCl, p^H 8, 10 mM MgCl₂, and 2 mM ADP[Et(PhNO₂)]). Middle trace: RIDS of 115 μ M W227Y mutant in ²H₂O buffer (100 mM Tris-HCl, p^H 8, 10 mM MgCl₂, and 2 mM ADP[Et(PhNO₂)]). Bottom trace: RIDS of 94 μ M W210,217,272Y mutant in ²H₂O buffer (100 mM Tris-HCl, p^H 8; 10 mM MgCl₂, 1.3 mM dithiothreitol, and 2 mM ADP[Et(PhNO₂)]). Asterisks indicate bands associated with the photolysis of caged ADP.

amino acid side-chain groups can also absorb in this region of the infrared spectrum (43). The 1515 and 1583 cm⁻¹ bands were associated respectively with the ring stretching of Tyr residues and the vibrational stretching of carboxylate of either Asp or Glu residues (44). The 1564 cm⁻¹ broad band, in the amide II region, was assigned mostly to the mixture of CN stretching and NH deformation modes, corresponding to buried NH groups whose protons have not been exchanged with deuterium of the solvent. The infrared spectrum of W210,217,272Y mutant (Figure 3) in the amide I region was slightly different from the infrared spectrum of wild-type CK (38). The shoulder at around 1632 cm⁻¹ was less pronounced in the infrared spectrum of W210,217,272Y mutant than in the infrared spectrum of wild-type CK. Otherwise the main amide I peak was located in the same position for these two spectra. Therefore one cannot exclude that a small part of mutant does not fold as the wild type.

ADP Binding Sites in Mutant CK and in Wild-Type CK. The reaction-induced infrared difference spectra (RIDS) of ADP[Et(PhNO₂)] in ²H₂O buffer containing W210,217,272Y mutant is shown in Figure 4 (bottom trace). The negative band at 1527–1528 cm⁻¹ and the positive band at 1685–1688 cm⁻¹ (indicated with asterisks in Figure 4) were

attributed respectively to the disappearance of the nitro group of ADP[Et(PhNO₂)] and the appearance of a carbonyl group of the photoproduct (45). Negative bands corresponded to vibrational modes of CK or ADP[Et(PhNO₂)] before illumination, while positive bands indicated vibrational modes related to the photoproducts or to the effects of Mg-ADP photorelease to CK. The three positive bands located at 1666, 1657, and 1637–1640 cm⁻¹ and the four negative bands located at 1648–1651, 1625, 1612–1615, and 1581–1584 cm⁻¹ resulted from the effects of photorelease of Mg-ADP in the presence of mutant CK. On the basis of earlier works (22, 33, 46), the 1666–1668, 1657–1660, 1648–1651, 1625–1626, and 1612 cm⁻¹ bands were assigned to carbonyl groups of peptide backbone adjacent to residues that can bind to the phosphate groups of the nucleotide moiety. The 1637–1640 cm⁻¹ band is attributed to a carbonyl group adjacent to residue that can interact with either the purine or ribose moieties of nucleotide. The 1648–1651, 1637–1640, and 1625–1626 cm⁻¹ component bands in the RIDS of wild-type creatine kinase are almost insensitive to isotopic shift induced by changing from ¹H₂O to ²H₂O buffers (46), suggesting that the carbonyl groups associated with these bands remained in the hydrophobic region. However, the 1612 cm⁻¹ band (deuterated buffer) shifted to 1615 cm⁻¹ (nondeuterated buffer), indicating an exposed carbonyl group (46). The 1581–1584 cm⁻¹ band is related to a carboxylate group of Asp or Glu that was affected during nucleotide binding. The infrared changes were relatively small and corresponded to the structural changes affecting 3–4 amino acid residues, based on the COBSI index of 0.0089 ± 0.0014 computed from the area of amide I bands (22, 47). In addition, the slight decrease of the amide II band, around 1560–1558 cm⁻¹, reflected an increasing exchange of protons of about 1–2 NH groups with deuterium of solvent, due to ADP binding. The RIDS of ADP[Et(PhNO₂)] in ²H₂O buffer, containing either wild-type CK (46) or W227Y mutant CK (22) are shown for comparison in Figure 4 (top and middle traces). The RIDS of W210,217,272Y mutant (Figure 4, bottom trace) is similar to the RIDS of wild type (Figure 4, top trace), except for the 1637–1640 cm⁻¹ positive band. The intensity of this band was reduced in the case of W210,217,272Y mutant as compared to that of wild type and to that of W227Y mutant. The intensities of the negative and positive bands in the RIDS of inactive W227Y mutant were much smaller as compared to the intensities of the corresponding bands of the RIDS of wild type except that the 1637 cm⁻¹ component band decreased moderately.

DISCUSSION

Nucleotide Binding Site in Wild-Type CK As Probed by Raman Spectroscopy. Raman spectroscopy is more sensitive than infrared spectroscopy for detecting structural changes that are directly related to the hydrophobic environment of Trp and Tyr residues (24). The unchanged position of Raman band at 1556 cm⁻¹ indicated that Trp residues remained in a hydrophobic environment upon nucleotide binding. As can be seen in Figure 1, no changes within uncertainties can be seen for Trp and Tyr. Although the intensity of intrinsic fluorescence decreased upon the addition of nucleotide, its maximum emission sensitive to the environment was not affected (Figure 2). These results taken together suggest that changes in Trp environment are negligible as probed by

Raman spectroscopy or by intrinsic Trp fluorescence. To monitor stacking interactions involving aromatic residues of protein and purine of nucleotide moiety, the nucleotide band located at 1310 cm^{-1} was used (48). It is well-established that stacking interactions of nucleic acid bases can diminish the Raman intensities associated with their ring vibrations (49–51). Raman measurements reveal a weak change around 1310 cm^{-1} in the spectrum of creatine kinase upon addition of Mg-ADP substrate in normal buffer (Figure 1). This change is due to a slight pH-dependent intensity variation of the 1310 cm^{-1} ADP band (52) rather to stacking interactions under dilute nucleotide concentrations. Thus Raman spectroscopy did not reveal putative stacking interactions involving purine of Mg-ADP with tyrosine or tryptophan residues of CK in our dilute nucleotide solutions.

Nucleotide Binding Site in Wild-Type CK and in Mutants As Probed by Infrared Spectroscopy. The reproducibility level of reaction-induced difference spectra in the amide I region is less than 0.1% (26), corresponding to an uncertainty of 0.44 residue (439–436 absorbing groups in mutants and in wild type: 380 carbonyl groups of peptide backbone and 18 Arg, 16 Asn, 12 Gln, and 13–10 Tyr side chain residues). ADP binding to CK or to W210,217,272Y induced very small infrared differences in the amide I region, corresponding to 3–4 amino acid residues affected by ADP binding to CK. On the other hand, conformational changes within nucleotides during their binding to CK were also observed by ^{13}C NMR spectra of 2- ^{13}C -labeled nucleotides. Significant differences in the cation Mn(II)-2C in CK–Mn-ATP and in CK–Mn-ADP complexes were observed (53). They were interpreted as conformational adjustment accompanying the interconversion of reactants and products in the active site.

The RIDS of wild type and of mutant W210,217,272Y were similar, except for the $1637\text{--}1640\text{ cm}^{-1}$ positive band, which was absent in the RIDS of mutant W210,217,272Y. This band was present in the RIDS of wild-type CK and Mg-ADP. It was tentatively assigned to a carbonyl group of the peptide backbone that was affected by the binding of purine or ribose moiety of ADP (22, 33) since this band was not observed in the RIDS of wild-type CK and P_i , ruling out interactions involving phosphate groups of nucleotide (46). We propose that the Mg-ADP binding to CK could be responsible for the slight changes of the peptide backbone carbonyl group adjacent to a tryptophan residue. This band was visible in the RIDS of the inactive mutant W227Y. Thus Trp227 cannot be solely responsible for the changes of infrared difference band located at $1637\text{--}1640\text{ cm}^{-1}$, suggesting that one of the remaining three tryptophan residues may be involved in this interaction. It is less likely that Trp210 could participate in nucleotide interaction since this Trp is at the monomer–monomer interface (30). Trp272 is located away from the putative binding site (8). Thus the carbonyl group adjacent to Trp217 is a good candidate for the spectral changes associated with the appearance of a positive $1637\text{--}1640\text{ cm}^{-1}$ band in the RIDS of wild-type CK (Figure 4).

Concluding Remarks. Two essential facts that are relevant to the mechanism of the reversible phosphoryl transfer from nucleotide to creatine emerged from this work:

(A) The putative roles of Trp residues in nucleotide binding to CK were clarified. More precisely, Raman measurements indicated that neither hydrogen bonding nor

environment of Trp residues (uncertainty of less than 0.2 residue) was affected during Mg-ADP binding. The hydrophobic environment of Tyr residues (uncertainty of 0.65 residue) was not altered upon Mg-ADP binding. Comparisons of infrared spectra of wild-type CK with those of inactive W227Y and active W210,217,272Y mutants indicated that Trp227 is not likely to participate in base-stacking interactions, although this residue is essential for the activity of CK. These results suggest that Trp227 can play a key role to prevent water molecules from entering in the active site as proposed earlier (21, 33). In addition, we suspect that another Trp, most probably Trp217, could be implicated in the Mg-ADP binding to CK, inferring that the putative base-stacking interaction (14), which was not detected by our Raman results, may involve this residue and that this type of interaction is not essential for the activity but it may help to steer nucleotide in the vicinity of the active site of CK.

(B) ADP binding to CK produced only minor changes in the secondary structure of CK, corresponding to secondary structure changes less than 1% (3–4 residues over 439–436 absorbing groups; uncertainty of 0.44 residue). This result should be compared with recent small-angle X-ray diffraction data (54, 55) and molecular modeling (56) indicating that Mg–nucleotide binding produced a decrease of the gyration radius of CK from 2.80 nm (free enzyme, so-called open conformation) to 2.56 nm (CK + MgATP, so-called closed conformation). Taken together, these results would indicate that the closure of the cleft where nucleotide is bound induced relatively large domain movement that is not accompanied by large secondary structure changes. It was already reported that large changes in the profile structure of Ca^{2+} -ATPase of sarcoplasmic reticulum can occur with only minor changes in the secondary structure of the Ca^{2+} -ATPase (27, 57, 58). Similar conclusions can be reached by comparing infrared (59) and small-angle X-ray diffraction (60) results for arginine kinase. It is tempting to generalize and to propose that domain movements caused by substrate binding to enzyme do not always involve large secondary structure changes and that local structural alterations are sufficient to promote large changes in the profile structure.

REFERENCES

1. Saks, V. A., Rosenshtraukh, L. V., Smirnov, V. N., and Chazov, E. I. (1978) *Can. J. Physiol. Pharmacol.* 56, 691–706.
2. Wallimann, T., Wyss, M., Brdiczka, D., Nicolay, K. and Eppenberger, H. M. (1992) *Biochem. J.* 281, 21–40.
3. Watts, D. C. (1973) in *The Enzymes* (Boyer, P. D., Ed.) Vol. VIII, pp 383–455, Academic Press, New York.
4. Bessman, S. P. and Carpenter, C. L. (1985) *Annu. Rev. Biochem.* 54, 831–862.
5. Mühlebach, S. M., Gross, M., Wirz, T., Wallimann, T., Perriard, J.-C., and Wyss, M. (1994) *Mol. Cell. Biochem.* 133/134, 245–262.
6. Suzuki, T., and Furukohori T. (1994) *J. Mol. Biol.* 237, 353–357.
7. Strong, S. J., and Ellington, W. R. (1995) *Biochim. Biophys. Acta* 1246, 197–200.
8. Fritz-Wolf, K., Schnyder, T., Wallimann, T., and Kabsch, W. (1996) *Nature* 381, 341–345.
9. Rao, J. K. M., Bujacz, G., and Wlodawer, A. (1998) *FEBS Lett.* 439, 133–137.

10. Zhou, G., Somasundaram, T., Blanc, E., Parthasarathy, G., Ross Ellington, W., Chapman, M. S. (1998) *Proc. Natl. Acad. Sci. U.S.A.* 95, 8449–8454.
11. Balny, C., Travers, F., Barman, T., and Douzou, P. (1985) *Proc. Natl. Acad. Sci. U.S.A.* 82, 7495–7499.
12. Roustan, C., Kassab, R., Pradel, L. A., and Van Thoai, N. (1968) *Biochim. Biophys. Acta* 167, 326–338.
13. Travers, F., and Barman, T. E. (1980) *Eur. J. Biochem.* 110, 405–412.
14. Kägi, J. H. R., Ting-Kai, L., and Vallee, B. L. (1971) *Biochemistry* 10, 1007–1015.
15. Price, N. C. (1972) *FEBS Lett.* 24, 21–23.
16. Vasák, M., Nagayama, K., Wüthrich, K., Mertens, M. L., and Kägi, J. H. R. (1979) *Biochemistry* 18, 5050–5055.
17. Messmer, C. H., and Kägi, H. R. (1985) *Biochemistry* 24, 7172–7178.
18. Zhou, H. M., and Tsou, C. L. (1985) *Biochim. Biophys. Acta* 830, 59–63.
19. Grossman, S. H. (1989) *Biochemistry* 28, 4894–4902.
20. Grossman, S. H., France, R. M., and Mattheis, J. R. (1992) *Biochim. Biophys. Acta* 1159, 29–36.
21. Gross, M., Furter-Graves, E. M., Wallimann, T., Eppenberger, H. M., and Furter, R. (1994) *Protein Sci.* 3, 1058–1068.
22. Raimbault, C., Perraut, C., Marcillat, O., Buchet, R., and Vial, C. (1997) *Eur. J. Biochem.* 250, 773–782.
23. Fleury, F., Ianoul, A., Kryukov, E., Sukhanova, A., Kudelina, I., Wynne-Jones, A., Bronstein, I. B., Maizieres, M., Berjot, M., Dodson, G. G., Wilkinson, A. J., Holden, J. A., Feofanov, A. V., Alix, A. J. P., Jardillier, J.-C., and Nabiev, I. (1998) *Biochemistry* 37, 14630–14642.
24. Raussens, V., Pézolet, M., Ruyschaert, J.-M., and Goormaghtigh, E. (1999) *Eur. J. Biochem.* 262, 176–183.
25. Hu, X., and Spiro, T. G. (1997) *Biochemistry* 36, 15701–15712.
26. Mäntele, W. (1993) *Trends Biochem. Sci.* 18, 197–202.
27. Cepus, V., Ulbrich, C., Allin, C., Trouiller, A., and Gerwert, K. (1998) *Methods Enzymol.* 291, 223–245.
28. Murali, N., Jarori, G. K., Landy, S. B., Nageswara Rao, B. D. (1993) *Biochemistry* 32, 12941–12948.
29. Mertens, M. L., and Kägi, H. R. (1979) *Anal. Biochem.* 96, 448–455.
30. Perraut, C., Clottes, E., Leydier, C., Vial, C., and Marcillat, O. (1998) *Proteins: Struct., Funct., Genet.* 32, 43–51.
31. Kunkel, T. A., Roberts, J. D., and Zakour, R. A. (1987) *Methods Enzymol.* 154, 367–382.
32. Glasoe, P. K., and Long, F. A. (1960) *J. Phys. Chem.* 64, 188–190.
33. Raimbault, C., Leydier, C., Vial, C. and Buchet, R. (1997) *Eur. J. Biochem.* 247, 1197–1208.
34. Siamwiza, M. N., Lord, R. C., Chen, M. C., Takamatsu, T., Harada, I., Matsuura H., and Shimanouchi, T. (1975) *Biochemistry* 14, 4870–4876.
35. Miura, T., Takeuchi, H., and Harada, I. (1988) *Biochemistry* 27, 88–94.
36. Thomas, G. J., Jr., Prescott, B., and Day, L. A. (1983) *J. Mol. Biol.* 165, 321–356.
37. Harada, I., Miura, T., and Takeuchi, H. (1986) *Spectrochim. Acta* 42A, 307–312.
38. Raimbault, C., Couthon, F., Vial, C., Buchet, R. (1995) *Eur. J. Biochem.* 234, 570–578.
39. Font, B., Vial, C., Goldschmidt, D., and Gautheron, D. (1981) *Arch. Biochem. Biophys.* 212, 195–203.
40. Krimm, S., and Bandekar, J. (1986) *Adv. Protein Chem.* 38, 181–364.
41. Byler, D. M., and Susi, H. (1986) *Biopolymers* 25, 469–487.
42. Surewicz, W. K., Mantsch, H. H., and Chapman, D. (1993) *Biochemistry* 32, 115–130.
43. Goormaghtigh, E., Cabiaux, V., and Ruyschaert, J. M. (1994) in *Physical Methods in the Study of Biomembranes* (Hilderson, H. J. and Ralston, G. B., Eds.) Vol. 23, pp 329–362, Plenum Press, New York.
44. Chirgadze, Y. N., Fedorov, O. V., and Trushina, N. P. (1975) *Biopolymers* 14, 679–694.
45. Barth, A., Corrie, J. E. T., Gradwell, M. J., Maeda, Y., Mäntele, W., Meier, T., and Trentham, D. R. (1997) *J. Am. Chem. Soc.* 119, 4149–4159.
46. Raimbault, C., Buchet, R., and Vial, C. (1996) *Eur. J. Biochem.* 240, 134–142.
47. Barth, A., von Germar, F., Kreutz, W., and Mäntele, W. (1996) *J. Biol. Chem.* 271, 30637–30646.
48. Weaver, J. L., and Williams, R. W. (1988) *Biochemistry* 27, 8899–8903.
49. Wen, Z. Q., Armstrong, A., and Thomas, G. J. (1999) *Biochemistry* 38, 3148–3156.
50. Peticolas, W. L., Kubashek, K. L., Thomas, G., and Tsuboi, M. (1987) in *Biological Applications of Raman Spectroscopy* (Spiro, T. G., Ed.) Vol. 1, pp 81–133, Wiley-Interscience, New York.
51. Nishimura, Y., Hirakawa, A. Y., and Tsuboi, M. (1978) in *Advances in Infrared and Raman Spectroscopy* (Clark, R. J. H., and Hester, R. E., Eds.) Vol. 5, pp 217–275, Heyden, London.
52. O'Connor, T., Johnson, C., and Scovell, W. M. (1976) *Biochim. Biophys. Acta* 447, 495–508.
53. Ray, B. D., Chau, M. H., Fife, W. K., Jarori, G. K., and Nageswara Rao, B. D. (1996) *Biochemistry* 35, 7239–7246.
54. Forstner, M., Kriechbaum, M., Laggner, P., and Wallimann, T. (1996) *J. Mol. Struct.* 383, 217–222.
55. Forstner, M., Kriechbaum, M., Laggner, P., and Wallimann, T. (1998) *Biophys. J.* 75, 1016–1023.
56. Zhou, G., Ellington, W. R., and Chapman, M. S. (2000) *Biophys. J.* 78, 1541–1550.
57. Martonosi, A. N. (1995) *Biosci. Rep.* 15, 263–281.
58. von Germar, F., Barth, A., and Mäntele, W. (2000) *Biophys. J.* 78, 1531–1540.
59. Raimbault, C., Besson, F., and Buchet, R. (1997) *Eur. J. Biochem.* 244, 343–351.
60. Dumas, C., and Janin, J. (1983) *FEBS Lett.* 153, 128–130.

BI000009D